5800–5811 *Nucleic Acids Research, 2008, Vol. 36, No. 18* *Published online 9 September 2008*
doi:10.1093/nar/gkn581

The putative RNase P motif in the DEAD box helicase Hera is dispensable for efficient interaction with RNA and helicase activity

Martin H. Linden[1], Roland K. Hartmann[2] and Dagmar Klostermeier[1,*]

[1]Department of Biophysical Chemistry, Biozentrum, University of Basel, Klingelbergstrasse 70, 4056 Basel, Switzerland and [2]Philipps-Universität Marburg, Institute for Pharmaceutical Chemistry, Marbacher Weg 6, 35037 Marburg, Germany

Received July 15, 2008; Revised and Accepted August 27, 2008

ABSTRACT

DEAD box helicases use the energy of ATP hydrolysis to remodel RNA structures or RNA/protein complexes. They share a common helicase core with conserved signature motifs, and additional domains may confer substrate specificity. Identification of a specific substrate is crucial towards understanding the physiological role of a helicase. RNA binding and ATPase stimulation are necessary, but not sufficient criteria for a *bona fide* helicase substrate. Here, we report single molecule FRET experiments that identify fragments of the 23S rRNA comprising hairpin 92 and RNase P RNA as substrates for the *Thermus thermophilus* DEAD box helicase Hera. Both substrates induce a switch to the closed conformation of the helicase core and stimulate the intrinsic ATPase activity of Hera. Binding of these RNAs is mediated by the Hera C-terminal domain, but does not require a previously proposed putative RNase P motif within this domain. ATP-dependent unwinding of a short helix adjacent to hairpin 92 in the ribosomal RNA suggests a specific role for Hera in ribosome assembly, analogously to the *Escherichia coli* and *Bacillus subtilis* helicases DbpA and YxiN. In addition, the specificity of Hera for RNase P RNA may be required for RNase P RNA folding or RNase P assembly.

INTRODUCTION

Structural rearrangements of RNA or RNA/protein complexes are required in a variety of key cellular processes involving RNA, from transcription, RNA editing, splicing and translation to RNA decay. These processes are generally facilitated by the action of numerous RNA helicases, enzymes that couple the energy of ATP hydrolysis to a structural rearrangement in their RNA or RNA/protein substrate (1). DEAD box helicases constitute the largest family of RNA helicases. They share a helicase core, comprising two RecA-like domains connected by a flexible linker that carries all signature motifs of DEAD box helicases (2). Additionally, flanking domains may target the helicase to its RNA substrate, either by high-affinity binding to a specific RNA, or by increasing the overall affinity by non-specific RNA binding. The RNA helicase YxiN from *Bacillus subtilis* binds specifically to hairpin 92 in the peptidyl transferase center of 23S ribosomal RNA (rRNA) *via* its C-terminal domain (CTD) (3,4). This domain adopts a canonical RNA recognition motif (RRM) fold, a αβ-sandwich with a four-stranded antiparallel β-sheet flanked by two α-helices (5). The *Escherichia coli* homolog of YxiN, DbpA, contains a homologous CTD that interacts with hairpin 92 of the *E. coli* 23S rRNA. For both helicases, unwinding of a double-stranded region adjacent to the hairpin 92 has been demonstrated (3,6), consistent with a role in ribosome biogenesis. In contrast, the DEAD box proteins Mss116p from yeast and Cyt-19 from *Neurospora crassa* carry basic CTDs (7) that mediate non-specific binding to a multitude of RNA structures (8–11). These basic CTDs preferentially interact with structured RNAs, and the helicase unwinds adjacent duplexes that are not tightly interacting with the structured part of the RNA (12). This binding mode has been suggested to allow for a general 'RNA chaperone' function of these helicases (7,12,13).

Hera, a DEAD box helicase from the thermophilic bacterium *Thermus thermophilus*, has been described almost 10 years ago as a 'heat-resistant RNA-dependent ATPase' (14). It consists of a helicase core (~370 aa) comprising all signature motifs of DEAD box helicases, and an additional CTD of ~140 aa (Figure 1). While we have recently determined the structure of the N-terminal RecA-like domain of the helicase core (aa 1–207) (15), no structural information is available for the remainder of the helicase. An initial qualitative characterization of Hera has shown

*To whom correspondence should be addressed. Tel: +41 61 267 2381; Fax: +41 61 267 2189; Email: dagmar.klostermeier@unibas.ch

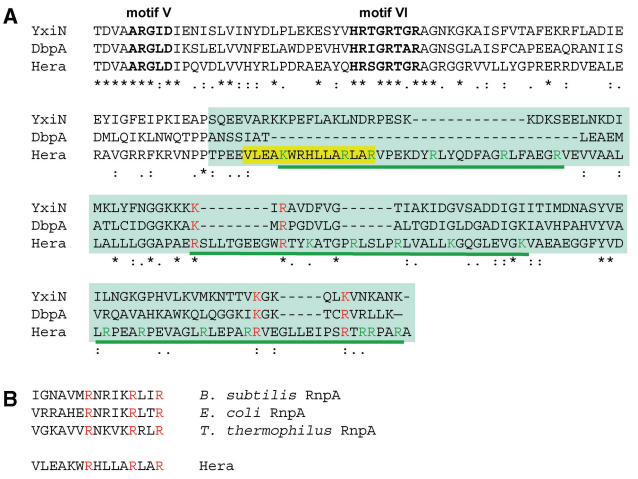

Figure 1. Hera constructs and sequence alignments. (**A**) Sequence alignment of the CTDs of *T. thermophilus* Hera, *E. coli* DbpA, and *B. subtilis* YxiN. The alignment was created with ClustalW. The CTD is highlighted in light green. Conserved positively charged residues are highlighted in red, positively charged residues in the Hera CTD are marked in green. The green bars indicate the N-terminal, center- and C-terminal regions with a slight clustering of positively charged residues in the Hera CTD. (**B**) Sequence comparison of the RNR-motif in RnpA from *E. coli*, *B. subtilis* and *T. thermophilus* with the RNase P motif in Hera. The three conserved arginines in the RNR motif are marked in red.

that its intrinsic ATPase activity is stimulated by a variety of nucleic acid substrates, including *T. thermophilus* RNase P RNA as well as 16S and 23S rRNA (14). For a Hera mutant lacking the C-terminal 146 residues, ATPase stimulation by RNase P RNA, but not by 16S rRNA, was reduced (14). The sequence of the Hera CTD does not share any similarities to the RRMs of YxiN or DbpA (Figure 1), or to the basic CTDs of Cyt-19 or Mss116p. Instead, it contains a 15 aa motif of weak similarity to the RNR-motif conserved in bacterial RNase P proteins (14). Bacterial RNase P, consisting of a catalytic RNA subunit (~380 nt) and a small basic protein (RnpA, ~120 aa), catalyzes tRNA 5′-end maturation (16,17). The RNR-motif in RnpA is involved in the interaction with the RNA component (18–20). The corresponding motif in Hera was therefore dubbed a 'putative RNase P motif' (14), and its involvement in RNase P RNA binding to Hera was suggested.

Identification of its RNA substrates is an important step towards defining a physiological role for a DEAD box helicase. We have recently shown that the *B. subtilis* DEAD box helicase YxiN undergoes a conformational change in response to cooperative binding of the 23S rRNA substrate and ATP (21). This closure of the inter-domain cleft within the helicase core leads to assembly of the ATPase sites and is thought to be a prerequisite for efficient RNA unwinding. To understand the substrate specificity and the function of the thermostable RNA helicase Hera, we have analyzed the ability of different nucleic acid substrates to induce a closure of the inter-domain cleft in single molecule fluorescence resonance energy transfer (smFRET) experiments. Hera adopts a closed conformation in the presence of Rnase P RNA, fragments of 23S rRNA, or polyU-RNA. A ribosomal RNA fragment comprising only hairpin 92 and an adjacent 9-bp helix is unwound by Hera in an ATP-dependent fashion. Remarkably, when the CTD of Hera was deleted, only polyU-RNA retained the capacity to induce a closed conformation of the helicase core, indicating that two mechanisms lead to activation of the Hera helicase core, either mediated by specific interactions of RNA with the CTD, or by non-specific RNA binding to the core itself. Simultaneous alanine substitutions of all three arginines within the putative RNase P motif did not abolish the conformational change in the presence of any of the RNA substrates, or the unwinding of the ribosomal RNA fragment. Thus, the putative RNase P motif can be excluded as a major determinant for Hera binding to RNA substrates, or for RNA unwinding.

MATERIALS AND METHODS

Cloning, mutagenesis, protein production and purification

The gene encoding Hera was amplified from *T. thermophilus* HB27 genomic DNA, and the PCR fragment was ligated into the NdeI/BamHI restriction sites of pET27b (Novagen). Primer sequences were 5′-GGAATTCCAT ATGGAGTTTA AAGACTTTCC CCTGAAGCCA GAA-3′ (Hera_for), and 5′-GGCGGATCCC TACGC CCTGG CCGG-3′ (Hera_rev).

Site-directed mutagenesis was performed according to the Quikchange protocol (Stratagene). The C-terminal deletion mutant Hera_core (aa 1–365) was constructed by introducing two stop codons after the codon for amino acid 365.

For production of the CTD of Hera (Hera_CTD,), the genomic region coding for amino acids 370–511 was amplified with primers 5′-GGGCCATGGA GGAGGT CCTC GAGGCC-3′ (Hera_d369_for) and Hera_rev, and cloned into the NcoI/BamHI restriction sites of pETM30 (G. Stier, EMBL Heidelberg). Correct sequences were confirmed for all constructs.

Proteins were produced in *E. coli* BL 21 (DE3) CodonPlus RIL or BL 21 (DE3) CodonPlus RP (Stratagene) or Rosetta (DE3) (Novagen). Bacteria were grown for 24 h at 37°C in auto-inducing medium (22), using a 5000-fold trace elements stock solution containing 50 mM $FeCl_3$, 20 mM, $CaCl_2$, 10 mM $MnCl_2$, 10 mM $ZnSO_4$, 2 mM $CoCl_2$, 2 mM $CuCl_2$, 2 mM $NiSO_4$, Na_2MoO_4, 2 mM Na_2SeO_3 and 2 mM H_3BO_3. Cells were disrupted with a microfluidizer in 50 mM Tris/HCl, pH 7.5, 500 mM NaCl (buffer A) in the presence of protease inhibitors (Roche). For cysteine-containing proteins, all buffers were supplemented with 2 mM β-mercaptoethanol (BME). All columns were from GE Healthcare.

Hera wild-type and mutants and Hera_core were purified at room temperature. The crude extract was incubated at 65°C for 10 min, and precipitated *E. coli* proteins were removed by centrifugation. From the supernatant, Hera was precipitated with 40% (w/v) ammonium sulphate on ice for 120 min. The precipitate was dissolved in buffer A and applied to a S200 16/60 size exclusion column equilibrated in the same buffer. Fractions containing the

respective protein were pooled, dialyzed over night at 4°C against 50 mM Tris/HCl, pH 7.5, 200 mM NaCl (buffer B) and applied to a 10 ml Heparin sepharose column equilibrated in buffer B. Elution was performed with a linear gradient of 200 mM to 2 M NaCl in buffer B. Fractions containing Hera were pooled, dialyzed overnight at 4°C against buffer B and applied to a 10 ml SP sepharose cation exchange column. Proteins were eluted with a linear salt gradient to 2 M NaCl in buffer B, and Hera containing fractions were pooled, concentrated and dialyzed overnight at 4°C against buffer A.

For purification of the CTD (Hera_CTD), the crude extract in buffer A was applied to a glutathione sepharose column and eluted with buffer A supplemented with 20 mM glutathione. The His_6-GST-Hera_CTD fusion protein was cleaved with TEV-protease during over night dialysis against buffer A. After adding 20 mM imidazole, the pool was applied to a Ni^+ column to remove non-cleaved fusion protein and the TEV protease. Elution was performed with buffer A containing 500 mM imidazole, and the fractions containing Hera_CTD were further purified on a S75 16/60 size exclusion column equilibrated in buffer A. To remove residual nucleic acids, the pool was dialyzed overnight at 4°C against buffer B and applied to a Q-sepharose column. Hera_CTD was in the flow through, which was concentrated and dialyzed over night at 4°C against buffer A.

Proteins were shock-frozen in liquid nitrogen and stored at −80°C. Concentrations were determined photometrically using the calculated extinction coefficients $\varepsilon = 33\,710\,M^{-1}\,cm^{-1}$ (Hera wild-type), $\varepsilon = 17\,210\,M^{-1}\,cm^{-1}$ (Hera_core), $\varepsilon = 16\,500\,M^{-1}\,cm^{-1}$ (Hera_CTD).

All Hera constructs eluted as dimers from a calibrated S200 size-exclusion column, with an apparent molecular weight for Hera of 104 kDa (calculated: 56.0 kDa), and 128 kDa for the mutant Hera_E115C/R260C and Hera_Rpm. The apparent molecular weight for Hera_core was 67 kDa (wt and cysteine mutant, calculated: 40.0 kDa), and 25 kDa for Hera_CTD (calculated: 15.5 kDa). Consistent with the thermophilic origin of Hera, all constructs were in the soluble fraction after 10 min incubation at 65°C. Yields of >95% pure protein (as judged from Coomassie-stained SDS–PAGE) were 10 mg/l cell culture (full length Hera), 10 mg/l (Hera_core) and 5 mg/l (Hera_CTD). *Escherichia coli* RnpA and *B. subtilis* YxiN were purified as described (23).

Adenine nucleotides and RNA and DNA substrates

Adenine nucleotides were purchased from Pharma Waldhof or JenaBioscience. PolyU-RNA (size range 100–1000 kDa) was from Sigma. The 153-mer RNA substrate comprising nucleotides 2483–2634 of the *B. subtilis* 23S rRNA was generated by T7 polymerase *in vitro* transcription as described (24). A 32/9-mer comprising hairpin 92 of the 23S rRNA was constructed by annealing a synthetic 32-mer and a synthetic 9-mer as described (24). *Thermus thermophilus* RNase P RNA (*T. thermophilus*) were generated by T7 polymerase *in vitro* transcription as described (25,26). As a single-stranded DNA substrate (ssDNA), the oligonucleotide 5′-GCCAGACCCT CCTC TTCGCC GCCGCCCTCC CCTCCTGGGC GAAAA GG-3′ was used. To obtain a double-stranded DNA substrate (dsDNA), the complementary strand was annealed.

ATPase assays

Steady-state ATP hydrolysis was monitored in a coupled enzymatic assay at 37°C via the decrease in A_{340} due to oxidation of NADH to NAD^+ (27) as described (24). Assay conditions were 50 mM Tris/HCl pH 7.5, 150 mM NaCl, 5 mM $MgCl_2$, 200 μM NADH, 400 μM phosphoenolpyruvate, 23 μg/ml lactate dehydrogenase, 36 μg/ml pyruvate kinase, 5 mM ATP and 1 μM or 100 nM Hera in the absence and presence of RNA substrate. Initial reaction velocities were calculated from the absorbance change $\Delta A_{340}/\Delta t$ using the extinction coefficient $\varepsilon_{340,\,NADH} = 6300\,M^{-1}\,cm^{-1}$.

RNA unwinding

Unwinding assays were performed with 5 μM of the 32/9-mer ribosomal RNA and 10 μM Hera in 50 mM Tris/HCl pH 7.5, 150 mM NaCl, 5 mM $MgCl_2$ at 25°C for 30 min, and products were analyzed by native PAGE as described (21,24).

Fluorescent labeling

Fluorescent labeling of cysteines was performed in 50 mM Tris/HCl, pH 7.5, 500 mM NaCl, 1 mM TCEP at a protein concentration of 30 μM with an 8-fold molar excess of Alexa488-maleimide (A488, donor) and Alexa546-maleimide (A546, acceptor) for 1 h at 25°C. The reaction was stopped by adding 100 mM BME, and free dye was removed by size exclusion chromatography on Micro Bio-Spin 30 columns (BioRad). Labeling efficiencies were determined from absorbance ratios at 493 nm (A488, corrected for A546 contributions) or 554 nm (A546) and 280 nm (protein, corrected for dye contributions).

Determination of quantum yields and Förster distances

Quantum yields ϕ of the donor A488 attached to Hera were determined as described (28) relative to fluorescein in 0.1 M NaOH ($\phi = 0.92$) (29).

Förster distances (30) were calculated from normalized absorbance spectra of acceptor-only labeled protein, normalized fluorescence spectra of the donor-only labeled protein, and the quantum yield of the donor as described (21). The orientation factor κ^2 was set to 2/3.

Single molecule FRET experiments

Single molecule FRET experiments were performed using a home-built confocal microscope as described (21). Only fluorescence bursts above a threshold of 100 photons were considered in the analysis. Measured background-corrected fluorescence intensities were corrected for crosstalk (α: donor crosstalk in acceptor channel, β: acceptor crosstalk in donor channel), different quantum yields and detection efficiencies of donor and acceptor fluorescence (γ), direct excitation of the acceptor (δ) and converted into FRET efficiencies as described (21). Measurements were

performed at room temperature (25°C) in 50 mM Tris/HCl, pH 7.5, 150 mM NaCl, 5 mM $MgCl_2$ with 50–100 pM fluorescently labeled protein (concentration of donor fluorophore), 3 mM nucleotide and 1 mM (nucleotides) poly-U RNA or 400 nM of other nucleic acids, unless stated otherwise.

RESULTS

Interaction of Hera with different RNA substrates: RNA-induced conformational changes

The *T. thermophilus* helicase Hera comprises a helicase core and an additional ~140 aa CTD. While various RNA molecules stimulate the intrinsic ATPase activity of Hera (14), the effect of these substrates on the ATPase rate and their affinity for Hera have not been determined, and the functional implications for Hera helicase activity are elusive. The *B. subtilis* DEAD box RNA helicase YxiN binds its specific RNA substrate, a region of the 23S rRNA, via its CTD adjacent to the helicase core (3,4). We have shown that complex formation between RNA substrates and YxiN in the presence of ATP [or the non-hydrolyzable analog 5′-adenylyl-β,γ-imidodiphosphate (ADPNP)] is coupled to a closure of the inter-domain cleft in the helicase core (21). This conformational change is a prerequisite for RNA unwinding and therefore provides a direct link to helicase function. As a consequence, it can be exploited as a probe to investigate substrate specificity. To identify potential nucleic acid substrates for the *T. thermophilus* DEAD box helicase Hera, we constructed a Hera mutant carrying one cysteine on each side of the inter-domain cleft in the helicase core (Hera_E115C/R260C), introduced donor (A488) and acceptor (A546) fluorophores, and performed single molecule FRET experiments (Figure 2). In the absence of ligands, FRET histograms for Hera_E115C/R260C showed a mean FRET efficiency (E_{FRET}) of 0.65–0.70, corresponding to an inter-dye distance of 4.5–4.7 nm (Förster distance: 5.2 nm). From the crystal structure of the DEAD box helicase DeaD from *Methanococcus jannaschii* (31), which shows good agreement with the open helicase core conformation of YxiN in solution (21), a slightly larger distance between the labeled residues of 5.5 nm is predicted, indicating a more compact conformation of the Hera helicase core in the absence of ligands compared to YxiN. Nevertheless, the experimental inter-dye distance is consistent with an open conformation of the Hera helicase core. The FRET efficiency was unaffected by binding of ADPNP (data not shown), confirming that binding of this non-hydrolyzable ATP analog alone does not induce a closure of the inter-domain cleft within the Hera helicase core.

The closed conformer of DEAD box helicases has been captured in crystal structures of the *Drosophila* helicase Vasa and the human eIF4A-III in complex with ADPNP and a 6- or 7-mer oligoU-RNA (32–34), indicating that in principle non-specific binding to a single-stranded RNA is sufficient to stimulate the closure of the cleft in the helicase core. In these structures, the distance between the residues corresponding to the labeled positions in Hera is 4.2 nm. When polyU-RNA was added to Hera/ADPNP, an increase in E_{FRET} to ~0.8 was seen, corresponding to a decrease of the inter-dye distance to 4.1 nm. PolyU-RNA binding to Hera/ADPNP thus promotes the formation of the closed Hera conformer with a similar domain arrangement as seen in other DEAD box helicases.

Next, we interrogated the interaction of Hera with more complex RNA molecules. A stimulation of the intrinsic ATPase activity of Hera by 16S and 23S rRNA has previously been reported (14). Despite the low sequence similarity between the CTDs of Hera and YxiN, a closure of the inter-domain cleft in Hera was detected with the YxiN substrate (Figure 2), a 153-mer comprising nucleotides 2483–2635 of the *B. subtilis* 23S rRNA [corresponding to the 154-mer reported in ref. (35), Supplementary Figure S1]. Similarly, the minimal bipartite 32/9-mer RNA substrate of YxiN and DbpA, consisting of hairpin 92 and flanked by a 5′-sequence that forms a 9-bp duplex with a 9-mer added *in trans*, promoted the formation of the closed conformer, confirming that Hera recognizes the same 23S rRNA structural element as YxiN and DbpA. The concentrations used in these experiments, together with the ~90% complex formation observed in the FRET histogram, provide an upper limit for the K_d of the Hera/RNA complex of 50 nM, consistent with high affinity binding to the ribosomal RNA. Interestingly, the FRET efficiency remained unchanged when only the 9-mer of the 32/9-mer substrate was added to Hera/ADPNP. However, in the presence of the 32-mer, a closure of the inter-domain cleft was detected (Figure 2D), clearly identifying hairpin 92 as the key determinant for the interaction of rRNA fragments with Hera.

Prompted by the proposal that the putative RNase P motif in the Hera CTD mediates specific binding to RNase P RNA (14), we performed smFRET experiments with Hera_E115C/R260C in the presence of RNase P RNA from *T. thermophilus* (379 nt, Supplementary Figure S1). Adding RNase P RNA to the Hera/ADPNP complex led to an increase of the FRET efficiency to ~0.85, demonstrating that RNase P RNA interacts with Hera and induces the closure of the cleft in the helicase core. The conformational change already occurs at RNA concentration of 50 nM, consistent with a K_d of ~10 nM. In contrast to the observations with the tested rRNA fragments, RNase P RNA, and polyU-RNA, Hera remained in the open conformation in the presence of a 47 nt ssDNA, or a 47 bp dsDNA (Figure 2B), suggesting that Hera is specific for RNA.

In summary, 23S rRNA-derived RNA fragments containing hairpin 92, RNase P RNA and polyU-RNA induce the formation of the active, closed Hera conformer. The 32-mer is the smallest substrate that elicits this specific conformational change.

Comparison of Hera and Hera_core

The CTDs of DEAD box helicases confer RNA-binding specificity to the helicase core, such as in YxiN or DbpA, or contribute to the overall affinity by non-specific RNA binding. The CTD of Hera lacks significant sequence

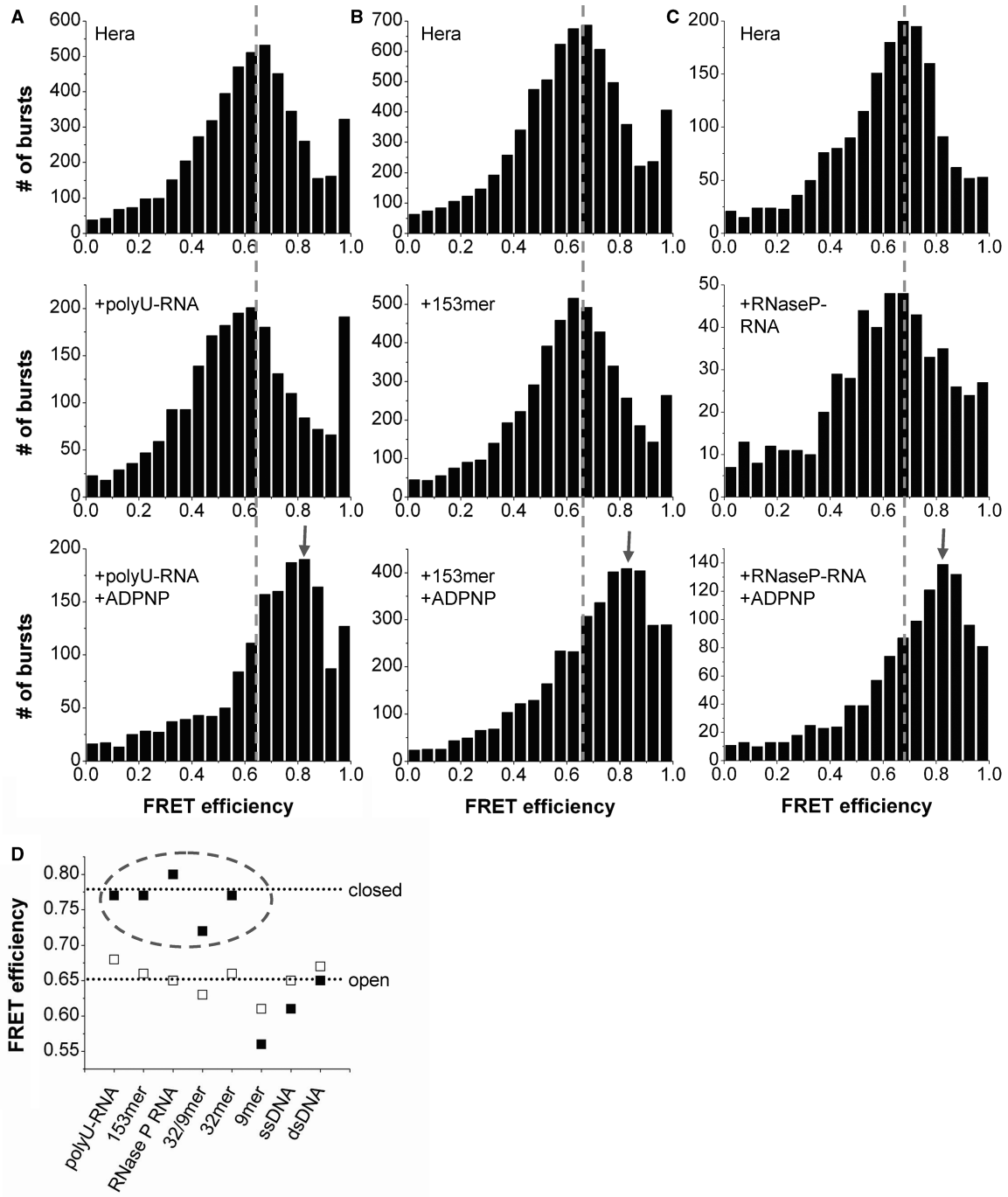

Figure 2. RNA-induced conformational changes in Hera. FRET histograms for Hera_E115C/R260C in the absence of RNA (top panels), in the presence of RNA (center panels) and in the presence of the respective RNA and ADPNP (bottom panels). (**A**) PolyU-RNA, (**B**) 153-mer rRNA and (**C**) RNase P RNA. The broken gray line marks the FRET efficiency for Hera. An increase in FRET efficiency from 0.65 to 0.8 is detected in the presence of all three RNAs and ADPNP (gray arrows), indicating a closure of the cleft within the Hera helicase domain in response to RNA and ADPNP binding. (**D**) Overview of FRET efficiencies for Hera_E115C/R260C in the presence of different nucleic acid substrates. Open squares: in the presence of nucleic acid only, closed squares: in the presence of nucleic acid and ADPNP. In the context of full-length Hera, polyU-RNA, RNase P RNA and the ribosomal RNA fragments induce a closure of the inter-domain cleft in the helicase core (circled).

similarity to the YxiN CTD or to the basic CTDs of the general chaperones Mss116p and Cyt-19. To dissect the role of the Hera CTD for RNA binding, we performed smFRET experiments with different nucleic acid substrates using a protein variant lacking the CTD (Hera_core, aa 1–365, Figure 3). The E_{FRET} for donor/acceptor labeled Hera_core in the absence of ligands was significantly lower than for the full-length enzyme (E_{FRET} Hera_core = 0.45–0.5, inter-dye distance 5.2–5.4 nm), and closer to the distance predicted from the *M. jannaschii* DEAD structure. This suggests that the cleft between the RecA-like domains is larger in Hera_core

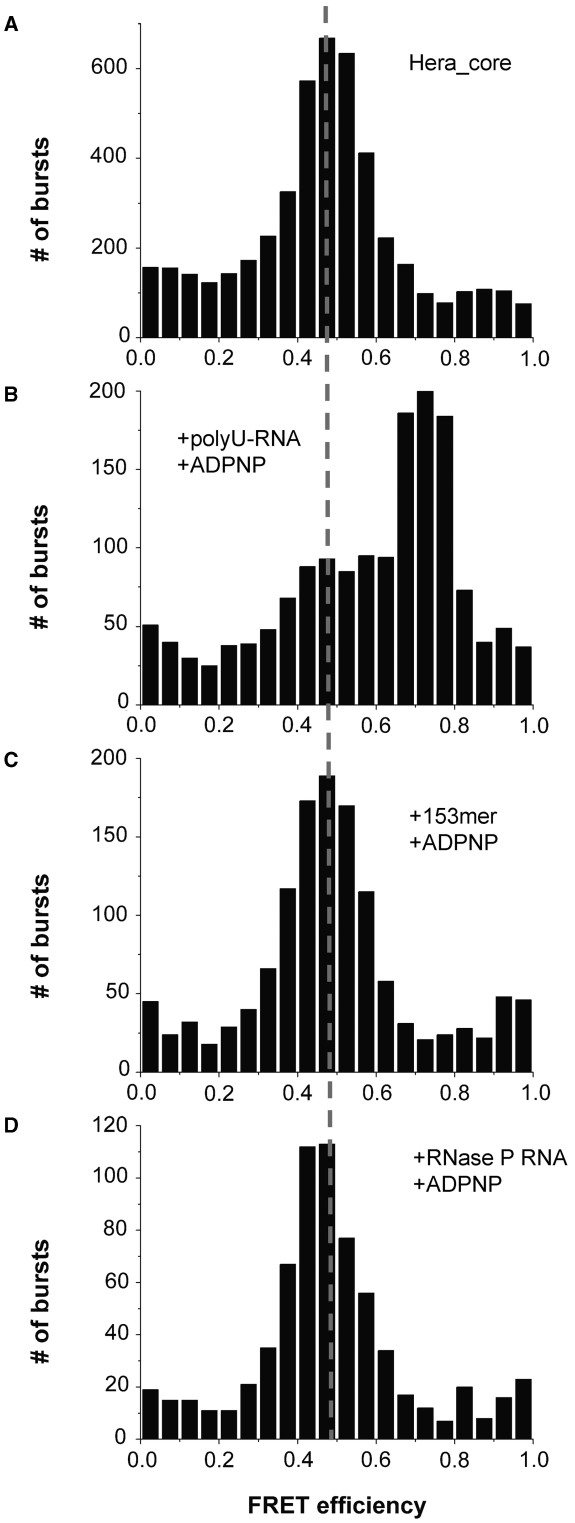

Figure 3. RNA-induced conformational changes in Hera_core. FRET histograms for Hera_core_E115C/R260C in the absence and presence of RNA. (**A**) No RNA, (**B**) polyU-RNA and ADPNP, (**C**) 153-mer and ADPNP and (**D**) RNase P RNA and ADPNP. The FRET efficiency of 0.50 in the absence of ligands (marked by the broken gray line) indicates a less compact conformation of the core compared to full-length Hera ($E_{FRET} = 0.65$). Only polyU-RNA induces the formation of the closed conformer ($E_{FRET} = 0.75$), whereas the FRET efficiency remains at 0.50 in the presence of the 153-mer or RNase P RNA, indicating that these RNAs do not elicit a conformational change in Hera_core.

compared to full-length Hera. Possibly, the CTD stabilizes a more compact conformation of the Hera helicase core.

As with full-length Hera, the 9-mer RNA, ssDNA, or dsDNA did not affect the E_{FRET}, consistent with Hera_core remaining in the open conformation when these nucleic acids are present. In contrast to full-length Hera, the 153-mer, the 32/9-mer, the 32-mer and RNase P RNA also did not influence the observed FRET efficiencies, demonstrating that the conformation of Hera_core was not affected by these RNAs. Only in the presence of polyU-RNA was an increase of the FRET efficiency observed ($E_{FRET} = 0.70$–0.75, corresponding to an inter-dye distance of 4.3–4.5 nm), indicative of the closure of the inter-domain cleft. This FRET efficiency is similar to that observed for full-length Hera, corroborating that the closed conformations of the helicase core are similar in Hera and Hera_core. These data pinpoint that the high affinity interaction of Hera with the ribosomal RNA fragments as well as with RNase P RNA are mediated by the CTD missing in Hera_core. In contrast, interaction with polyU-RNA is a property of the helicase core. In conclusion, the switch to the closed conformer can be achieved by two mechanisms. One is intrinsic to the core itself, and can be induced by binding of non-specific RNA, and the second is mediated by specific RNA binding to the CTD, and most likely involves simultaneous interaction of the same RNA with the helicase core.

Consistent with the smFRET results, the intrinsic ATPase activity of Hera was stimulated by RNase P RNA, the 153-mer and polyU-RNA (Figure 4), but not by ssDNA, or dsDNA. The intrinsic ATP hydrolysis by Hera is characterized by a k_{cat} of $7 \times 10^{-3}\,s^{-1}$. This rate constant is increased 260-fold in the presence of RNase P RNA, and 190-fold in the presence of the 153-mer, respectively. PolyU-RNA also strongly stimulated ATP

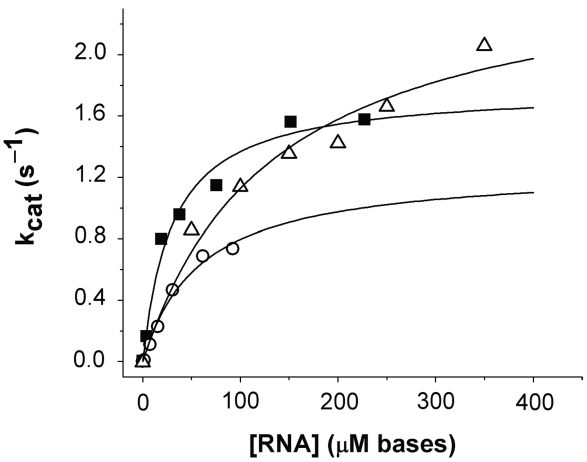

Figure 4. ATPase stimulation of Hera by nucleic acid substrates. Hera is a Michaelis–Menten enzyme. The intrinsic ATPase activity is characterized by a k_{cat} value of $7 \times 10^{-3}\,s^{-1}$. RNase P RNA (squares), the 153-mer (open circles) and polyU-RNA (open triangles) stimulate the intrinsic ATPase activity of Hera. The Michaelis–Menten constants are: $k_{cat} = 1.8\,s^{-1}$, $K_{M,app} = 77$ nM (29 μM nucleotides, RNase P RNA), $k_{cat} = 1.3\,s^{-1}$, $K_{M,app} = 390$ nM (59 μM nucleotides, 153-mer) and $k_{cat} = 2.6\,s^{-1}$, $K_{M,app} = 134$ μM (nucleotides, polyU-RNA), corresponding to a 190- to 370-fold ATPase stimulation.

hydrolysis significantly (370-fold). The $K_{M,app}$ values (77 nM/29 μM nucleotides, RNase P RNA, 390 nM/59 μM nucleotides, 153-mer, and 134 μM nucleotides for polyU-RNA) are larger than the K_d values estimated from smFRET experiments and most likely do not merely reflect binding but contain contributions from ATP hydrolysis. In contrast to full-length Hera, the intrinsic ATPase activity of Hera_core was only stimulated by polyU-RNA (to a similar extent as the full-length helicase), but not by RNase P RNA or the ribosomal RNA fragments (Supplementary Figure S2). Together with our smFRET results, these findings demonstrate a direct correlation between the RNA-stimulated ATPase activity of a helicase and the formation of its closed conformer.

Complementation experiments of Hera_core with Hera_CTD provided *in trans* were unsuccessful, indicating that the CTD has to be present in *cis* to contribute to specific RNA substrate binding to Hera. The lack of complementation is consistent with reports on the *B. subtilis* helicase YxiN, where the CTD was also found to be incapable of presenting the RNA substrate to the helicase core (4).

The fact that polyU-RNA induces a closure of the inter-domain cleft in Hera_core, but specific interactions with RNase P RNA or the ribosomal 153-mer RNA fragment are lost upon deletion of the CTD demonstrates that Hera substrates interact with (at least) two distinct binding sites, one on the CTD, and one on the helicase core. Mechanistically, binding of structured RNA to the CTD may present RNA substrates to the helicase core in an orientation that permits unwinding, reminiscent of the function of the basic CTDs in the general 'RNA chaperone' DEAD box helicases.

No competition of Hera and RnpA for RNase P RNA

Footprinting, cross-linking and modification interference data define an interaction site for RnpA on RNase P RNA, involving the P2-J2/3-J3/4-P4-J18/2 region (cf. Supplementary Figure S1) in the catalytic core (19,36–38). Participation of the putative RNase P motif in the interaction of Hera with RNase P RNA implies that Hera binds to the same site on the RNase P RNA as RnpA, and a competition between Hera and RnpA would thus be predicted. Therefore, we addressed the question whether Hera and RnpA contact the same or overlapping binding sites on RNase P RNA in competition experiments (Figure 5). Cross-species complementation between different RNase P RNAs and RnpA proteins has been demonstrated in general (16,23,39,40), and specifically for *T. thermophilus* RNase P RNA and *E. coli* RnpA used here (41). Donor/acceptor-labeled Hera (50 pM) was incubated with 3 mM ADPNP and 50 nM *T. thermophilus* RNase P RNA, a concentration sufficient to induce the closure of the inter-domain cleft, and 200 nM *E. coli* RnpA (4-fold excess over Rnase P RNA) was added. The buffer conditions were very similar to the conditions under which the formation of an active RNase P from *E. coli* RnpA and *T. thermophilus* RNase P RNA has been demonstrated (41). FRET histograms showed a FRET efficiency of ~0.75 before and after RnpA addition (data not shown), demonstrating that Hera remained in the

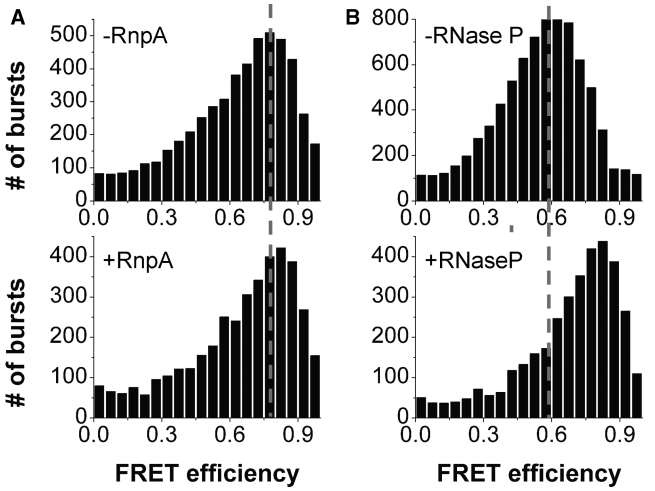

Figure 5. No competition of RnpA and Hera for RNase P RNA. (**A**) FRET histograms for Hera_E115C/R260C, 50 nM unlabeled Hera, 50 nM RNase P RNA and 3 mM ADPNP in the absence (upper panel) and in the presence (lower panel) of *E. coli* RnpA (1 μM). (**B**) The FRET efficiency in the absence of RnpA (marked by the gray broken line) is indicative of the Hera/RNase P RNA/ADPNP complex with a closed conformation of the helicase core. It is unaffected by the addition of RnpA, indicating that RnpA does not compete with Hera for RNase P RNA. (**B**) FRET histograms for Hera_E115C/R260C and 3 mM ADPNP in the absence (upper panel) and in the presence (lower panel) of preformed RnpA/RNase P RNA complex (50 nM RNase P RNA, 1 μM RnpA). The FRET efficiency in the absence of RnpA/RNase P (gray broken line) indicates the open conformation. Upon addition of the preformed RnpA/RNase P complex, Hera binds to the RNase P RNA and adopts the closed conformation.

closed conformation in the presence of RnpA, and RnpA was not able to compete with Hera for RNase P RNA binding under these conditions. To exclude that the remaining few RNase P RNA molecules not bound to RnpA in equilibrium are sufficient to remain bound to the low (picomolar) concentration of donor/acceptor-labeled Hera, we added 50 nM unlabeled Hera, and increased the concentration of RnpA to 1 μM (20-fold excess over Hera and RNase P RNA). However, the FRET efficiency again remained unchanged (Figure 5A), indicating that Hera retained its closed conformation and did not compete with RnpA for RNase P RNA binding. There are three possible explanations for this lack of competition: (i) Hera binds to the same site on RNase P RNA as RnpA, but with a significantly higher affinity, (ii) the RNase P RNA bound to Hera/ADPNP is trapped and does not or only very slowly dissociate, providing a kinetic hindrance for competition, or (iii) Hera and RnpA interact with different sites on RNase P RNA, and the formation of a ternary Hera/RNase P RNA/RnpA complex is possible.

The equilibrium dissociation constants of RnpA/RNase P RNA complexes are in the low nanomolar range (42–44) rendering it highly unlikely that 50 pM Hera can compete with 200 nM RnpA (4000-fold excess) for RNase P RNA binding due to a higher RNA affinity. To exclude a slow RNA dissociation as the reason for a lack of competition, we preincubated RNase P RNA (50 nM) and RnpA (1 μM), and added the preformed complex to donor/acceptor-labeled Hera (Figure 5B). Here, the FRET efficiency increased from ~0.6 to ~0.85

upon addition of the RNase P RNA/RnpA complex, clearly demonstrating that Hera binds to the RNase P RNA and adopts a closed conformation even when the preformed RNase P RNA/RnpA complex is added. These findings confirm that RnpA does not compete with Hera for RNase P RNA and suggests that Hera and RnpA contact different regions of RNase P RNA, thus rendering the formation of a ternary complex Hera/RNase P RNA/RnpA complex possible.

Role of the putative RNase P motif

Our experiments unambiguously assign the interaction site with RNase P RNA and rRNA fragments to the CTD of Hera. To confirm that the interaction with RNase P RNA is specific for Hera, we performed a reverse smFRET experiment with the donor/acceptor-labeled *B. subtilis* helicase YxiN, RNase P RNA and ADPNP (Figure 6). Here, RNase P RNA did not induce a closure of the inter-domain cleft, indicating that the interaction with RNase P RNA cannot be mediated by the RRM domain of YxiN.

The putative RNase P motif in the Hera CTD, ^{372}VLEAKWRHLLARLAR^{386}, has been suggested to confer binding specificity to RNase P RNA (14). To examine the role of this putative RNase P motif for RNA binding to Hera, we generated a triple mutant R378A/R383A/R386A (mutated arginines are underlined in the sequence above), termed Hera_Rpm, and tested this mutant for interactions with RNA in smFRET experiments (Figure 7A). As expected, polyU-RNA was still able to induce a conformational change in the helicase core of Hera_Rpm, providing a positive control for functionality of the helicase core. Surprisingly, both the 153-mer rRNA fragment and RNase P RNA promoted the closure of the inter-domain cleft in Hera_Rpm, indicating that the putative RNase P motif is dispensable for specific interactions with RNase P RNA. Both RNase P RNA and the 153-mer induced the conformational change even at low concentrations (50 and 400 nM, respectively), demonstrating that the affinity of Hera_Rpm for these substrates is not significantly reduced. Consistent with the observed conformational change in Hera_Rpm in response to RNase P RNA and 153-mer RNA binding, the ssATPase activity of Hera_Rpm was efficiently stimulated by both RNA molecules (Figure 7B). With 1.0 s^{-1} (RNase P RNA) and 1.4 s^{-1} (153-mer), the RNA-stimulated k_{cat} values were similar to those of wild-type Hera (1.8 and 1.3 s^{-1}, respectively). The $K_{M,app}$ values for the RNA substrates also remained unchanged (26 nM for RNase P RNA, 210 nM for the 153-mer, compared to 77 and 386 nM for full-length Hera). Hence, the removal of these three arginines which are conserved in the RNR-motif of RNase P proteins does not lead to a loss in RNA affinity for Hera for the substrates tested. These findings suggest that the presence of this sequence in Hera is purely coincidental and not functionally related to the RNR motif of RNase P.

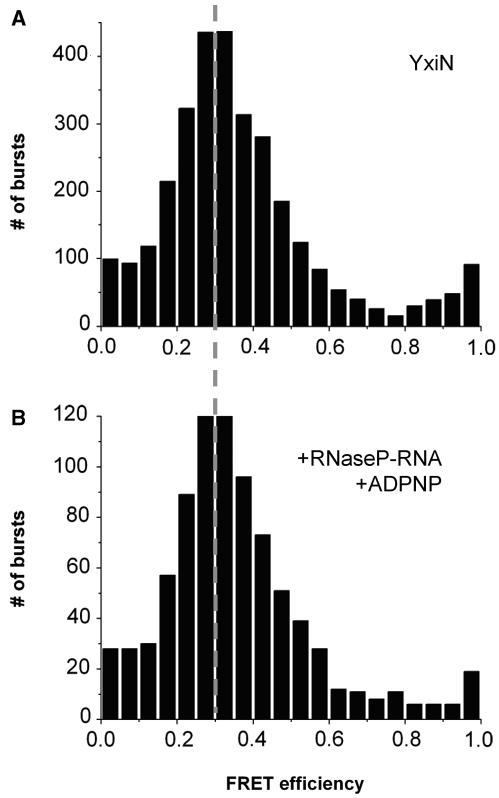

Figure 6. No interaction of RNase P RNA with *B. subtilis* YxiN. FRET histograms for YxiN_C61/267A_A115/S229C in the absence of ligands (upper panel) and in the presence (bottom panel) of RNase P RNA and ADPNP. The FRET efficiency of ~0.3 in the absence of RNase P RNA is indicative of the open YxiN conformation (21) and remains unchanged upon addition of RNase P RNA.

Hera is a functional RNA helicase

The observation that a 153-mer derived from the 23S ribosomal RNA, a 32/9-mer, and the isolated 32-mer, but not the 9-mer induce a conformational change in the Hera helicase core allows to assign the interaction site on the RNA to hairpin 92. The same hairpin is specifically recognized by the *E. coli* and *B. subtilis* DEAD box helicases DbpA and YxiN. This raises the question whether Hera may adopt a similar function in ribosome biogenesis to YxiN and DbpA, despite the lack of sequence homology between the CTDs of Hera and DbpA/YxiN. Therefore, we tested if the 32/9-mer can be unwound by Hera (Figure 8). Indeed, we observed 90% unwinding after 30 min incubation of the RNA with Hera in the presence, but not in the absence of ATP. Thus, Hera is a *bona fide* RNA helicase even at the non-physiological temperature of 25°C. In contrast, no RNA unwinding was detected with Hera_core, corroborating that the interaction of the ribosomal RNA with the CTD is essential for unwinding. Hera_Rpm, on the other hand, unwound the RNA substrate in the presence of ATP to a similar extent as wild-type. Thus, the RNase P-like motif is not only dispensable for RNA binding, but also for RNA helicase activity.

Altogether, Hera binds to RNase P RNA and to fragments of 23S rRNA via its CTD. Hera does not compete with RnpA for RNase P RNA binding, indicating that Hera and RnpA contact different regions on this RNA molecule. When three arginine residues in the putative RNase P motif in the Hera CTD are mutated to

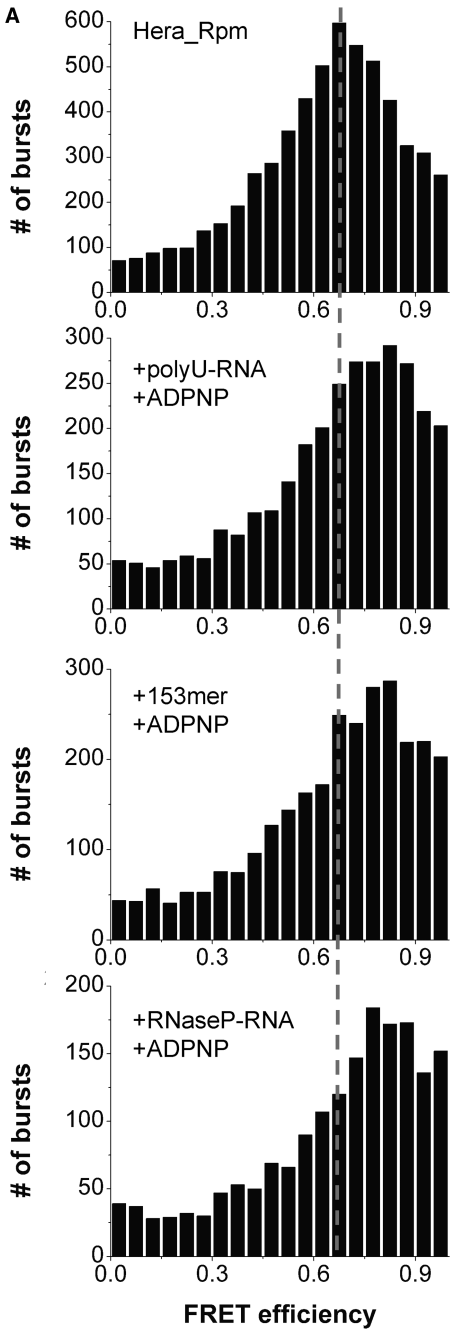

Figure 7. The RNase P motif mutant still interacts with RNase P RNA and the ribosomal 153-mer. (**A**) FRET histograms of Hera_Rpm_E115C/E260C in the absence of nucleic acids, and in the presence of 1 mM polyU-RNA, 400 nM of the 153-mer ribosomal RNA fragment, or 400 nM RNase P RNA and 3 mM ADPNP. All RNAs induce a conformational change in Hera_Rpm, demonstrating that the RNase P motif in Hera is not required for the interaction with these RNA substrates. The FRET efficiency of the open conformer is marked by a gray broken line. (**B**) RNA stimulation of the Hera_Rpm steady state ATPase activity by RNase P RNA (squares) and the 153-mer (open circles). The Michaelis–Menten parameters are $k_{cat} = 1.0\,s^{-1}$, $K_{M,app} = 26$ nM (10 μM nucleotides, RNase P RNA), $k_{cat} = 1.4\,s^{-1}$ and $K_{M,app} = 210$ nM (32 μM nucleotides, 153-mer). Hence, the ATPase activity of the Hera mutant carrying three mutations in the putative RNase P motif is still efficiently stimulated by RNase P RNA and the 153-mer.

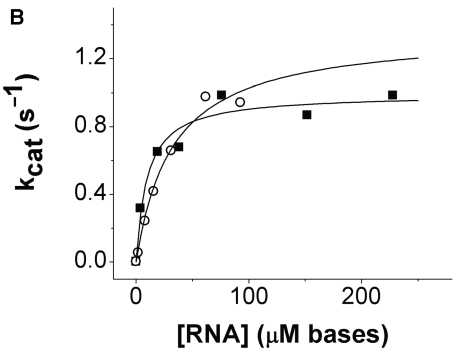

Figure 7. Continued.

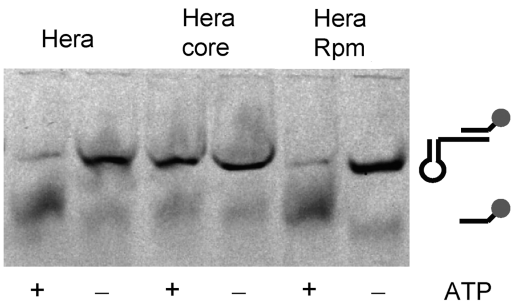

Figure 8. RNA unwinding by Hera, Hera_core and Hera_Rpm. A total of 5 μM of the 32/9-mer rRNA were incubated with 10 μM Hera, Hera_core or Hera_Rpm in the absence or presence of 5 mM ATP at 25°C for 30 min, and products were separated on a 15% polyacrylamide gel. Hera unwinds ~90% of the substrate in the presence of ATP, whereas no unwinding is observed in the absence of ATP. Hera_core is not able to unwind this RNA. Hera_Rpm shows ATP-dependent RNA unwinding activity with the same extent (90%) as wild-type Hera. The RNase P motif is thus dispensable for the helicase activity of Hera.

alanines, RNase P RNA and ribosomal RNA still interact with Hera, elicit a conformational change, and stimulate ATP hydrolysis. Our observations therefore argue against a specific role of this motif in RNase P RNA recognition, and against a primary role of this motif for RNA recognition and unwinding by Hera in general. A 32/9-mer that is a specific substrate for ribosome assembly-related bacterial helicases YxiN and DbpA is unwound by Hera and Hera_Rpm in an ATP-dependent fashion, confirming that Hera is a functional RNA helicase.

DISCUSSION

RNA substrates that induce the closed Hera conformation contain stem-loop structures

By monitoring the conformational change in the helicase core of Hera in response to RNA and ADPNP binding, we could define RNase P RNA and fragments of the 23S rRNA encompassing hairpin 92 (153-mer, 32/9-mer and 32-mer) as specific activators of the *T. thermophilus* RNA helicase Hera. The smallest RNA that elicits the formation of a closed Hera conformer is the 32-mer that consists of hairpin 92 of 23S rRNA, flanked by a 15-nt single-stranded region, suggesting that RNA recognition by Hera requires stem-loop structures. Based on their

accessibility in the tertiary structure, elements P3, P12 and possibly P2 (Supplementary Figure S1) are possible candidates for Hera binding to RNase P RNA (45).

The ATP-dependent unwinding of the 32/9-mer is proof that Hera is a *bona fide* RNA helicase. The fact that Hera, as YxiN and DbpA, binds the 23S rRNA-derived hairpin 92 and unwinds a flanking double-stranded region in an ATP-dependent fashion suggests that all three DEAD box helicases are involved in ribosome biogenesis. However, Hera also accepts RNase P RNA as a substrate, whereas YxiN is unresponsive to RNase P RNA. Together with the lack of sequence similarity between the CTDs of YxiN/DbpA and Hera this implies a different structural basis for RNA recognition.

Potential RNA interaction sites in the Hera CTD

The observation of the ATPase stimulation by RNase P RNA stimulated the search for RNA-binding motifs in Hera, and led to the proposal of the putative RNase P (RNR) motif in the CTD of Hera (14). The role of individual arginines in the RNR motif for interaction of RnpA with RNase P RNA has been tested in genetic complementation studies with *E. coli* RnpA mutants (46). Individual arginine-to-alanine exchanges within or close to the RNR motif did not compromise RNase P activity *in vivo*, but complementation was lost upon combining two of these mutations. In contrast, we could demonstrate here that a Hera triple mutant lacking all three conserved arginines of the RNase P motif remained fully responsive to activation by RNase P RNA and rRNA fragments, establishing that this motif is not a major determinant for the interaction of Hera with these RNA substrates. The Hera_CTD contains 24 positively charged residues, spread rather uniformly across the CTD sequence, which could be involved in RNA binding (cf. Figure 1A). It should be noted that the Hera CTD does not bear any sequence homology to the hydrophilic basic CTDs of the general 'RNA chaperones' Mss116p or Cyt-19, which are enriched in arginines, asparagines and glycines. The Hera CTD contains no asparagines, only few serines, but a large fraction of hydrophobic residues. These differences suggest a different structure and a different role of the Hera CTD, and argue against a similar function to provide unspecific binding to a large number of different RNAs. Compared to YxiN and DbpA, the CTD of Hera contains one larger and three smaller insertions (Figure 1A). This may be a consequence of its dual role: different regions of the CTD may be responsible for interactions with ribosomal RNA, and with RNase P RNA. Further deletion and mutagenesis studies will be required to identify the RNA determinants for binding to Hera and the residues of the Hera CTD involved in interactions with RNAs.

Does the interaction with RNase P RNA indicate a specialized function for Hera?

The observation that RNase P RNA binds with high affinity to Hera and elicits a conformational change in the Hera helicase core suggests that the interaction with RNase P RNA may be of functional relevance *in vivo*. Possibly, Hera may have evolved the capacity to interact with RNase P RNA in addition to rRNA to ascertain the assembly of functional RNaseP in *T. thermophilus*. A BLAST search of the UniProt database with the Hera CTD sequence retrieves only one significant hit: a 591 amino acid putative DEAD box helicase (Q1J0S9) from *Deinococcus geothermalis*, which, as a member of the *Deinococcus–Thermus* group, is a close relative of *T. thermophilus*. The genomic sequence of *D. radiodurans* also codes for a homologous putative DEAD box protein (DR_1624). An alignment of the complete proteins (Supplementary Figure S3) reveals a significant sequence conservation of the helicase core, also covering regions outside the helicase signature motifs, suggesting that these proteins might indeed be functionally related. The similarities between the CTDs are mainly restricted to the central region, with few conserved residues in the N- and C-terminal regions. Strikingly, and consistent with the lack of relevance for RNA binding to Hera, the putative RNase P motif is absent in the *Deinococcus* homologs.

While we currently cannot exclude a general function in RNA folding for Hera, its specific, high affinity interaction with RNase P RNA strongly suggests a functional role of Hera for RNase P. One possible role could be an 'RNA chaperone' function, with Hera promoting native folding of this G/C-rich thermostable RNase P RNA (47). Recent folding studies with RNase P RNA from *E. coli* have revealed that the RNA depends on correct transcriptional pauses for proper folding (48). Thus, Hera might be involved in cotranscriptional folding of RNase P RNA in *T. thermophilus*. In addition, the *T. thermophilus* and *Deinococcus* RnpA proteins are extended by 40–50 aa compared to other bacterial RnpAs (49), and the *Deinococcus* RNase P RNA is longer than other bacterial RNase P RNAs, suggesting unusual features of the *Thermus–Deinococcus* RnpA/RNase P RNA complexes. Assembly of these holoenzymes may be assisted by Hera-like RNA helicases.

The activation of Hera in response to RNase P RNA suggests a functional role for Hera in RNase P RNA folding or RNase P assembly. Clearly, future studies will have to identify the recognition elements within Hera and RNase P RNA, and define a minimal RNase P-derived substrate for Hera. The demonstration of ATP-dependent unwinding of an RNase P RNA structural element by Hera, as demonstrated here for the rRNA, would provide strong support for a specific role of Hera in RNase P RNA folding or RNase P assembly.

SUPPLEMENTARY DATA

Supplementary Data are available at NAR Online.

ACKNOWLEDGEMENTS

We thank Ines Hertel, Ramona Heissmann and Dominik Helmecke for technical assistance; Anne Karow for donor/acceptor labeling of the RNA helicase YxiN; Anke Henne for providing *T. thermophilus* HB27 genomic DNA; and Markus Rudolph for discussions.

FUNDING

VolkswagenStiftung (to D.K.); the Swiss National Science Foundation (to D.K.); and the Deutsche Forschungsgemeinschaft (to R.K.H). The Open Access publication charge for this article has been waived by Oxford University Press. NAR Editorial Board members are entitled to one free paper per year in recognition of their work on behalf of the journal.

Conflict of interest statement. None declared.

REFERENCES

1. Cordin,O., Banroques,J., Tanner,N.K. and Linder,P. (2006) The DEAD-box protein family of RNA helicases. *Gene*, **367**, 17–37.
2. Gorbalenya,A.E. and Koonin,E.V. (1993) Helicases: amino acid sequence comparisons and structure-function relationships. *Curr. Opin. Struct. Biol.*, **3**, 419–429.
3. Kossen,K., Karginov,F.V. and Uhlenbeck,O.C. (2002) The carboxy-terminal domain of the DExDH protein YxiN is sufficient to confer specificity for 23S rRNA. *J. Mol. Biol.*, **324**, 625–636.
4. Karginov,F.V., Caruthers,J.M., Hu,Y., McKay,D.B. and Uhlenbeck,O.C. (2005) YxiN is a modular protein combining a DEx(D/H) core and a specific RNA-binding domain. *J. Biol. Chem.*, **280**, 35499–35505.
5. Wang,S., Hu,Y., Overgaard,M.T., Karginov,F.V., Uhlenbeck,O.C. and McKay,D.B. (2006) The domain of the Bacillus subtilis DEAD-box helicase YxiN that is responsible for specific binding of 23S rRNA has an RNA recognition motif fold. *RNA*.
6. Pugh,G.E., Nicol,S.M. and Fuller-Pace,F.V. (1999) Interaction of the Escherichia coli DEAD box protein DbpA with 23 S ribosomal RNA. *J. Mol. Biol.*, **292**, 771–778.
7. Mohr,G. and Del Campo,M. (2008) Function of the C-terminal domain of the DEAD-box protein Mss116p analyzed in vivo and in vitro. *J. Mol. Biol.*, **375**, 1344–1364.
8. Halls,C., Mohr,S., Del Campo,M., Yang,Q., Jankowsky,E. and Lambowitz,A.M. (2007) Involvement of DEAD-box proteins in group I and group II intron splicing. Biochemical characterization of Mss116p, ATP hydrolysis-dependent and -independent mechanisms, and general RNA chaperone activity. *J. Mol. Biol.*, **365**, 835–855.
9. Grohman,J.K., Campo,M.D., Bhaskaran,H., Tijerina,P., Lambowitz,A.M. and Russell,R. (2007) Probing the mechanisms of DEAD-box proteins as general RNA chaperones: the C-terminal domain of CYT-19 mediates general recognition of RNA. *Biochemistry*, **46**, 3013–3022.
10. Mohr,S., Matsuura,M., Perlman,P.S. and Lambowitz,A.M. (2006) A DEAD-box protein alone promotes group II intron splicing and reverse splicing by acting as an RNA chaperone. *Proc. Natl Acad. Sci. USA*, **103**, 3569–3574.
11. Huang,H.R., Rowe,C.E., Mohr,S., Jiang,Y., Lambowitz,A.M. and Perlman,P.S. (2005) The splicing of yeast mitochondrial group I and group II introns requires a DEAD-box protein with RNA chaperone function. *Proc. Natl Acad. Sci. USA*, **102**, 163–168.
12. Tijerina,P., Bhaskaran,H. and Russell,R. (2006) Nonspecific binding to structured RNA and preferential unwinding of an exposed helix by the CYT-19 protein, a DEAD-box RNA chaperone. *Proc. Natl Acad. Sci. USA*, **103**, 16698–16703.
13. Mohr,S., Stryker,J.M. and Lambowitz,A.M. (2002) A DEAD-box protein functions as an ATP-dependent RNA chaperone in group I intron splicing. *Cell*, **109**, 769–779.
14. Morlang,S., Weglohner,W. and Franceschi,F. (1999) Hera from Thermus thermophilus: the first thermostable DEAD-box helicase with an RNase P protein motif. *J. Mol. Biol.*, **294**, 795–805.
15. Rudolph,M.G., Heissmann,R., Wittmann,J.G. and Klostermeier,D. (2006) Crystal structure and nucleotide binding of the Thermus thermophilus RNA helicase Hera N-terminal domain. *J. Mol. Biol.*, **361**, 731–743.
16. Guerrier-Takada,C., Gardiner,K., Marsh,T., Pace,N. and Altman,S. (1983) The RNA moiety of ribonuclease P is the catalytic subunit of the enzyme. *Cell*, **35**, 849–857.
17. Hartmann,E. and Hartmann,R.K. (2003) The enigma of ribonuclease P evolution. *Trends Genet.*, **19**, 561–569.
18. Brown,J.W. and Pace,N.R. (1992) Ribonuclease P RNA and protein subunits from bacteria. *Nucleic Acids Res.*, **20**, 1451–1456.
19. Buck,A.H., Kazantsev,A.V., Dalby,A.B. and Pace,N.R. (2005) Structural perspective on the activation of RNAse P RNA by protein. *Nat. Struct. Mol. Biol.*, **12**, 958–964.
20. Niranjanakumari,S., Day-Storms,J.J., Ahmed,M., Hsieh,J., Zahler,N.H., Venters,R.A. and Fierke,C.A. (2007) Probing the architecture of the B. subtilis RNase P holoenzyme active site by cross-linking and affinity cleavage. *RNA*, **13**, 521–535.
21. Theissen,B., Karow,A.R., Kohler,J., Gubaev,A. and Klostermeier,D. (2008) Cooperative binding of ATP and RNA induces a closed conformation in a DEAD box RNA helicase. *Proc. Natl Acad. Sci. USA*, **105**, 548–553.
22. Studier,F.W. (2005) Protein production by auto-induction in high density shaking cultures. *Protein Expr. Purif.*, **41**, 207–234.
23. Wegscheid,B. and Hartmann,R.K. (2006) The precursor tRNA 3′-CCA interaction with Escherichia coli RNase P RNA is essential for catalysis by RNase P in vivo. *RNA*, **12**, 2135–2148.
24. Karow,A.R., Theissen,B. and Klostermeier,D. (2007) Authentic interdomain communication in an RNA helicase reconstituted by expressed protein ligation of two helicase domains. *FEBS J.*, **274**, 463–473.
25. Busch,S., Kirsebom,L.A., Notbohm,H. and Hartmann,R.K. (2000) Differential role of the intermolecular base-pairs G292-C(75) and G293-C(74) in the reaction catalyzed by Escherichia coli RNase P RNA. *J. Mol. Biol.*, **299**, 941–951.
26. Heide,C., Pfeiffer,T., Nolan,J.M. and Hartmann,R.K. (1999) Guanosine 2-NH2 groups of Escherichia coli RNase P RNA involved in intramolecular tertiary contacts and direct interactions with tRNA. *RNA*, **5**, 102–116.
27. Adam,H. (1962) In Bergmeyer,H.U.(Hrsg.), *Methoden der Enzymatischen Analyse*. Verlag Chemie, Weinheim, pp. 573–577.
28. Parker,C.A. and Rees,W.T. (1960) Correction of fluorescence spectra and measurement of fluorescence quantum efficiency. *Analyst*, **85**, 587–600.
29. Magde,D., Wong,R. and Seybold,P.G. (2002) Fluorescence quantum yields and their relation to lifetimes of rhodamine 6G and fluorescein in nine solvents: improved absolute standards for quantum yields. *Photochem. Photobiol.*, **75**, 327–334.
30. Förster,T. (1959) Transfer mechanisms of electronic excitation. *Discuss. Faraday Soc.*, **27**, 7–17.
31. Story,R.M., Li,H. and Abelson,J.N. (2001) Crystal structure of a DEAD box protein from the hyperthermophile Methanococcus jannaschii. *Proc. Natl Acad. Sci. USA*, **98**, 1465–1470.
32. Sengoku,T., Nureki,O., Nakamura,A., Kobayashi,S. and Yokoyama,S. (2006) Structural basis for RNA unwinding by the DEAD-box protein Drosophila Vasa. *Cell*, **125**, 287–300.
33. Andersen,C.B., Ballut,L., Johansen,J.S., Chamieh,H., Nielsen,K.H., Oliveira,C.L., Pedersen,J.S., Seraphin,B., Le Hir,H. and Andersen,G.R. (2006) Structure of the exon junction core complex with a trapped DEAD-box ATPase bound to RNA. *Science*, **313**, 1968–1972.
34. Bono,F., Ebert,J., Lorentzen,E. and Conti,E. (2006) The crystal structure of the exon junction complex reveals how it maintains a stable grip on mRNA. *Cell*, **126**, 713–725.
35. Kossen,K. and Uhlenbeck,O.C. (1999) Cloning and biochemical characterization of Bacillus subtilis YxiN, a DEAD protein specifically activated by 23S rRNA: delineation of a novel sub-family of bacterial DEAD proteins. *Nucleic Acids Res.*, **27**, 3811–3820.
36. Biswas,R., Ledman,D.W., Fox,R.O., Altman,S. and Gopalan,V. (2000) Mapping RNA-protein interactions in ribonuclease P from Escherichia coli using disulfide-linked EDTA-Fe. *J. Mol. Biol.*, **296**, 19–31.
37. Rox,C., Feltens,R., Pfeiffer,T. and Hartmann,R.K. (2002) Potential contact sites between the protein and RNA subunit in the Bacillus subtilis RNase P holoenzyme. *J. Mol. Biol.*, **315**, 551–560.
38. Tsai,H.Y., Masquida,B., Biswas,R., Westhof,E. and Gopalan,V. (2003) Molecular modeling of the three-dimensional structure of the bacterial RNase P holoenzyme. *J. Mol. Biol.*, **325**, 661–675.

39. Waugh,D.S. and Pace,N.R. (1990) Complementation of an RNase P RNA (rnpB) gene deletion in Escherichia coli by homologous genes from distantly related eubacteria. *J. Bacteriol.*, **172**, 6316–6322.
40. Gossringer,M. and Hartmann,R.K. (2007) Function of heterologous and truncated RNase P proteins in Bacillus subtilis. *Mol. Microbiol.*, **66**, 801–813.
41. Marszalkowski,M., Willkomm,D.K. and Hartmann,R.K. (2008) Structural basis of a ribozyme's thermostability: P1-L9 interdomain interaction in RNase P RNA. *RNA*, **14**, 127–133.
42. Talbot,S.J. and Altman,S. (1994) Kinetic and thermodynamic analysis of RNA-protein interactions in the RNase P holoenzyme from Escherichia coli. *Biochemistry*, **33**, 1406–1411.
43. Day-Storms,J.J., Niranjanakumari,S. and Fierke,C.A. (2004) Ionic interactions between PRNA and P protein in Bacillus subtilis RNase P characterized using a magnetocapture-based assay. *RNA*, **10**, 1595–1608.
44. Cuzic,S. and Hartmann,R.K. (2007) A 2′-methyl or 2′-methylene group at G + 1 in precursor tRNA interferes with Mg2+ binding at the enzyme-substrate interface in E-S complexes of E. coli RNase P. *Biol. Chem.*, **388**, 717–726.
45. Torres-Larios,A., Swinger,K.K., Pan,T. and Mondragon,A. (2006) Structure of ribonuclease P–a universal ribozyme. *Curr. Opin. Struct. Biol.*, **16**, 327–335.
46. Jovanovic,M., Sanchez,R., Altman,S. and Gopalan,V. (2002) Elucidation of structure-function relationships in the protein subunit of bacterial RNase P using a genetic complementation approach. *Nucleic Acids Res.*, **30**, 5065–5073.
47. Hartmann,R.K. and Erdmann,V.A. (1991) Analysis of the gene encoding the RNA subunit of ribonuclease P from T. thermophilus HB8. *Nucleic Acids Res.*, **19**, 5957–5964.
48. Wong,T.N., Sosnick,T.R. and Pan,T. (2007) Folding of noncoding RNAs during transcription facilitated by pausing-induced nonnative structures. *Proc. Natl Acad. Sci. USA*, **104**, 17995–18000.
49. Feltens,R., Gossringer,M., Willkomm,D.K., Urlaub,H. and Hartmann,R.K. (2003) An unusual mechanism of bacterial gene expression revealed for the RNase P protein of Thermus strains. *Proc. Natl Acad. Sci. USA*, **100**, 5724–5729.